AIP | Applied Physics Letters

In-situ scanning electron microscopy and atomic force microscopy Young's modulus determination of indium oxide microrods for micromechanical resonator applications

Javier Bartolomé, Pedro Hidalgo, David Maestre, Ana Cremades, and Javier Piqueras

Citation: Applied Physics Letters **104**, 161909 (2014); doi: 10.1063/1.4872461
View online: http://dx.doi.org/10.1063/1.4872461
View Table of Contents: http://scitation.aip.org/content/aip/journal/apl/104/16?ver=pdfcov
Published by the AIP Publishing

In-situ scanning electron microscopy and atomic force microscopy Young's modulus determination of indium oxide microrods for micromechanical resonator applications

Javier Bartolomé, Pedro Hidalgo, David Maestre, Ana Cremades,[a] and Javier Piqueras
Departamento de Física de Materiales, Facultad de Ciencias Físicas, Universidad Complutense de Madrid, Ciudad Universitaria s/n, 28040 Madrid, Spain

(Received 12 March 2014; accepted 9 April 2014; published online 25 April 2014)

Electric field induced mechanical resonances of In_2O_3 microrods are studied by *in-situ* measurements in the chamber of a scanning electron microscope. Young's moduli of rods with different cross-sectional shapes are calculated from the resonance frequency, and a range of values between 131 and 152 GPa are obtained. A quality factor of 1180–3780 is measured from the amplitude-frequency curves, revealing the suitability of In_2O_3 microrods as micromechanical resonators. The Young's modulus, E, of one of the rods is also measured from the elastic response in the force-displacement curve recorded in an atomic force microscope. E values obtained by *in-situ* scanning electron microscopy and by atomic force microscopy are found to differ in about 8%. The results provide data on Young's modulus of In_2O_3 and confirm the suitability of *in-situ* scanning electron microscopy mechanical resonance measurements to investigate the elastic behavior of semiconductor microrods. © *2014 AIP Publishing LLC*. [http://dx.doi.org/10.1063/1.4872461]

The study of mechanical properties of low dimensional semiconductor structures, such as micro- and nanowires, nanobelts, and other elongated nanostructures, has gained in interest in the past years due to their application in the fabrication of cantilever-like micromechanical sensors,[1] flexible devices, micro and nanoelectromechanical systems (MEMS and NEMS) such as electromechanical nanoswitches,[2] mass sensors,[3] or in studies of the light-matter interaction through optomechanical coupling,[4,5] which could lead to optically-enhanced quality factor mechanical resonators.[6,7] Different techniques such as those based on electric field induced mechanical resonance, nanoindentation, or atomic force microscopy (AFM) have been used to determine the Young's modulus, E, of small structures. Some of these techniques are discussed for semiconducting and metallic nanowires in Ref. 8. In the particular case of semiconductor oxides, most of the previous reports refer to ZnO nanowires. *In-situ* transmission electron microscopy (TEM)[9] and scanning electron microscopy (SEM)[10] enabled to measure the resonance frequency of ZnO nanowires under an applied alternating electric field and to evaluate their elastic modulus. Agrawal *et al*. have reported a quantitative *in-situ* TEM tensile testing technique to measure accurately the Young's modulus of ZnO nanowires based on MEMS technology.[11] The Young's modulus of ZnO nanobelts has also been measured with an AFM by a modulated nanoindentation method[12] and by means of bending tests in an AFM.[13] Besides ZnO, the elastic modulus of small elongated structures of oxides has been scarcely reported, e.g., Ref. 14 on CuO and Ref. 15 on composite SiO_2/SiC wires, and no data on other oxides of technological interest are available. Among them, In_2O_3 exhibits large electrical conductivity, high transparency in the visible range and demonstrated resonant optical modes in elongated microstructures,[16,17] which, combined with its good chemical stability, makes it a suitable material for many of the above mentioned applications. In this work, the elastic properties of indium oxide microrods have been investigated by *in-situ* SEM measurements of resonance frequency and by AFM. The aim of the work was to obtain information on the Young's modulus of the structures and to analyze and compare the data obtained by the two experimental techniques used. To this purpose, measurements were performed by both techniques in the same microrod. The elastic modulus of the microrods, which have cross-sectional dimensions of few microns and lengths of up to the millimetre range, is not expected to depend on their size, shape, or aspect ratio, as such dependence has been found to be significant only for much smaller wires or rods.[10–12] However, in order to check this possibility and to obtain a representative value of the Young's modulus, mechanical resonance measurements were carried out in microrods with different shapes, as hexagonal and rectangular cross-sections. The obtained E values for In_2O_3 microrods are in the approximate range 131–152 GPa and demonstrate that both used techniques yield results without significant differences.

In_2O_3 microrods were synthesized by a thermal method with In_2S_3 powder as precursor. The powder was compacted to form discs, which were located onto an alumina boat and annealed under argon flow at 950 °C for 10 h. During the treatment, the precursor decomposes into In and S_2 and, since the furnace is not sealed for vacuum conditions, In_2O_3 forms by slow oxidation of indium. The disc acts as a source and simultaneously as a substrate for the growth of In_2O_3 micro- and nanostructures with different sizes and shapes.[17] The structures used in this work are microrods with lateral dimensions of several microns and lengths of hundreds of microns.

For the study of mechanical resonances, single In_2O_3 microrods were separated from the substrate, and one of the

[a]Author to whom correspondence should be addressed. Electronic mail: cremades@fis.ucm.es

ends was glued with silver paint onto a piece of n-Si (100) so that the rods were overhanging. The silicon substrate was glued to a copper electrode in front of a second electrode which is covered by a deposited gold layer as shown in Fig. 1(a). The set of sample and electrodes was placed in the chamber of a Fei Inspect SEM with the overhanging rods perpendicular to the electron beam.

Figure 1(b) shows a secondary electron low magnification image of substrate and electrode. An oscillating voltage with tunable frequency was applied with a Standford Research System SR830 DSP Lock-in amplifier, and a DC bias was generated by a Keithley 2400 SourceMeter. The amplitude of the oscillating rod as a function of the voltage frequency was measured from the images on the SEM screen. The frequency was tuned to find the resonance of the oscillating rod, and the Young's modulus was then determined from the elasticity theory as described below. Fifteen rods have been measured following the procedure described in this section. The obtained results are consistent, and, for the sake of clarity, we report detailed measurements for rods named as A, B, and C, which are representative of the different kinds of rod geometries studied. The AFM measurements were performed in air with a Nanotech microscope controlled by Dulcinea system and with a Si cantilever. Force–displacement curves were recorded in the contact mode on microrods mounted on a silicon substrate as described for the resonance measurements. The calibration of the Si cantilevers has been carried out with a diamond substrate by the following procedure: several force-displacement curves were recorded on the diamond substrate in order to relate the voltage signal of the photodiode to the real deformation of the cantilever, assuming that the diamond surface is not indented. This voltage-deformation conversion factor is then transformed into a voltage-force conversion factor by using the cantilever's elastic constant, which has been previously calibrated using its resonance frequency and geometric parameters, and Hooke's law. In the force-displacement curves of the Si-In_2O_3 system, the elastic deformation by indentation of the cantilever tip on the In_2O_3 has been estimated to be in the range of 0.1–2 nm for the range of used forces $F = 1$–100 nN, following the Herzt model for elastic deformations[18] and taking the values for the Poisson coefficients and Young Modulus of Si and In_2O_3 from Refs. 18 and 19, respectively. Therefore, the deformation by indentation has been neglected in our system.

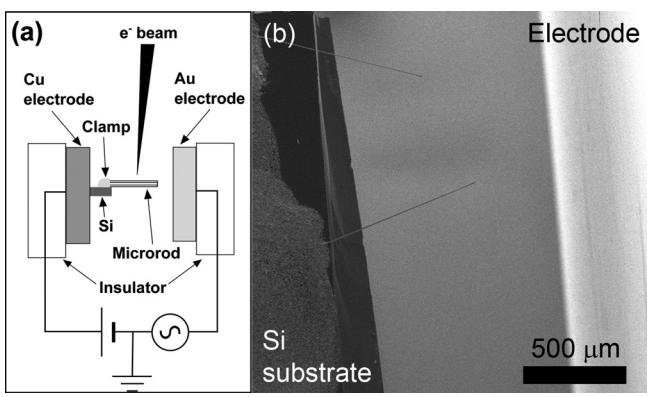

FIG. 1. (a) Experimental setup for *in-situ* scanning electron microscopy mechanical resonance measurements. (b) Secondary electron image of a microrod, showing the substrate and the counterelectrode.

The diameters of the nanostructures previously studied by *in-situ* TEM were of the order of ten or few tens of nanometers, which is a suitable size for the observation of the oscillation amplitudes in TEM. In the case of In_2O_3 microrods, the large chamber of SEM appears more adequate to perform the resonance experiments. By applying a constant potential between the electrodes, the rods are charged, and the electrostatic force causes the deflection of the microrod (see supplementary material).[20] In the case of an alternating potential, an alternating force appears, and oscillations of the microrods with the potential frequency take place (see supplementary material). By tuning the frequency of the applied field, an amplitude peak is measured at the resonance frequency of the microrod. From elasticity theory,[21] the fundamental resonance frequency of a rod of constant section is

$$\nu_i = \frac{\beta_i^2}{2\pi L^2}\sqrt{\frac{EI}{\rho S}}, \tag{1}$$

where β_i is a constant for the i-th harmonic, L the length of the rod, E the Young's modulus, I the second moment of inertia, ρ the density, and S the cross-sectional area.

Since the section is not always constant along the studied rods, it is necessary to introduce a correction factor, so that, after solving for E, Eq. (1) can be rewritten as

$$E = \frac{\nu_i^2 4\pi^2 L^4 \rho S_B}{I_B \alpha^2}, \tag{2}$$

where S_B and I_B are the section and the second moment of inertia at the base of the rods, and α is the correction factor, which depends on the geometry of the rod.[21] The shape of the rods, measured by SEM, has been approximated to a linear decrease of both their section and second moment of inertia according to the following equations:

$$S = S_B\left(1 - c\frac{x}{L}\right), \tag{3}$$

$$I = I_B\left(1 - c\frac{x}{L}\right), \tag{4}$$

where x is the distance from the fixed end to a point of the rod and c is a fitting parameter. Equations (3) and (4) imply some restrictions in the shape of the rods, which do not exactly match to the microrods of this work but, as described below, the results obtained by this approximation are consistent. The resonance frequency was measured in an almost constant hexagonal cross-section rod, labeled A, and compared with those obtained in variable hexagonal or rectangular cross-section rods, labeled B and C, respectively. Their geometric parameters, as well as the correction factor derived from the data provided in Ref. 21, are summarized in Table I.

Figures 2(a) and 2(b) show low magnification secondary electron images of the rod A, both in static condition and vibrating at a resonance frequency of $\nu = 1965.8$ Hz. Figure 2(c) shows the corresponding frequency versus amplitude

TABLE I. Physical parameters obtained from the electric field induced mechanical resonance measurements. L is the total length of the microrods, c is fitted parameter of the microrods section measurements to Eq. (3), ν_n is the resonance frequency along the n principal axis of vibration, E is the Young's modulus, and Q is the quality factor.

	Microrod		
	A	B	C
Cross section	Hexagonal	Hexagonal	Rectangular
Growth direction	[111]	[111]	[100]
L (μm)	1330 ± 10	1010 ± 10	782 ± 10
S_B (μm^2)	22.79 ± 0.32	25.4 ± 1.6	31.6 ± 2.5
c	0.03 ± 0.10	0.84 ± 0.11	0.897 ± 0.072
α	3.515	4.992	6.279
ν_1 (Hz)	1955.5 ± 0.1	4938 ± 1	$11\,682 \pm 1$
ν_2 (Hz)	1965.8 ± 0.1	5015 ± 1	$11\,770 \pm 1$
E_1 (GPa)	150 ± 11	141 ± 11	151 ± 9
E_2 (GPa)	152 ± 11	146 ± 11	131 ± 8
Q_1	$(3.78 \pm 0.14) \times 10^3$	$(2.17 \pm 0.42) \times 10^3$	$(1.18 \pm 0.26) \times 10^3$
Q_2	$(2.23 \pm 0.10) \times 10^3$	$(1.80 \pm 0.28) \times 10^3$	$(1.17 \pm 0.18) \times 10^3$

curve, with two resonance peaks at 1955.5 and 1965.8 Hz, respectively, and the theoretical curve fitting to the equation for the amplitude of a damped harmonic oscillator:

$$y_0 = \frac{C}{\sqrt{\left(\nu_i^2 - \nu^2\right)^2 + 4\nu^2\gamma^2}}, \tag{5}$$

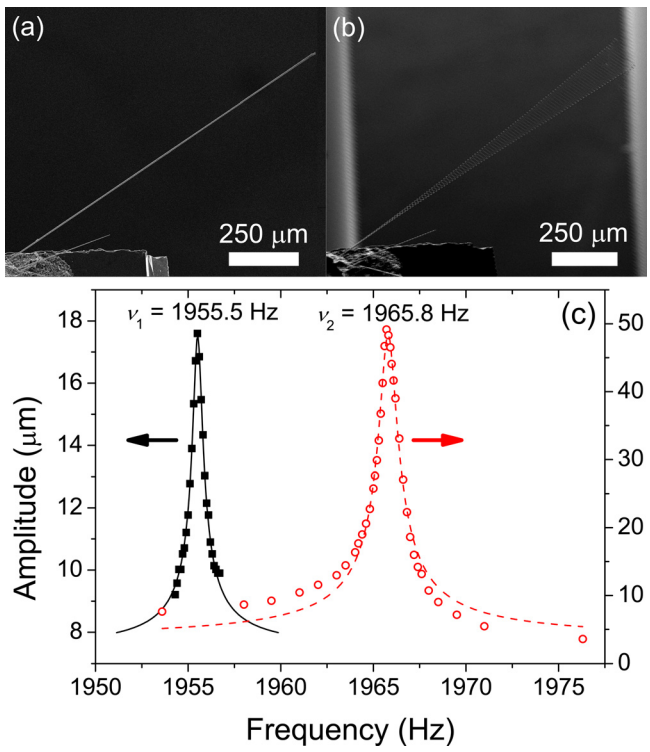

FIG. 2. (a) and (b) Low magnification secondary electron images of the microrod A in static condition and vibrating at a resonance frequency of $\nu_2 = 1965.8$ Hz. (c) Mechanical resonance curve of the same microrod with two peaks corresponding to the resonance in the two principal axes of vibration. Solid and dashed lines correspond to the best fit to a damped harmonic oscillator equation.

where C is a constant, ν is the applied frequency, and γ is the attenuation factor. The maximum amplitude is obtained for $\nu \sim \nu_i$, when the attenuation is small. The fit shows a good agreement with the experimental curves. The appearance of the two peaks is due to resonance frequencies in the two principal axes of vibration. Young's modulii obtained from Eq. (2) and resonance frequencies measured for each rod type are indicated in Table I. Calculated values spread in the range between 131 to 152 GPa, with a mean value of 145 GPa. It is to be noticed that in the application of Eq. (2), the α value is subject to errors arising from the measurements of the cross section along the microrod, which can lead to different E values. Nevertheless, differences between the estimated E moduli of the rods are, in general, less than 10%. There are scarce reports on In_2O_3 Young's modulus determination, even for bulk material. In Ref. 22, an E value of 105 GPa was reported for In_2O_3 thick films measured by dynamical nanoindentation, while a Young's modulus of 206 GPa can be derived from the theoretically calculated values of the elastic constants reported in Ref. 23. From the bulk modulus experimentally measured in Ref. 24, and the one calculated by the local density approximation in Ref. 25, a Young's modulus of 210 and 187 GPa, respectively, can be derived for In_2O_3 using a Poisson ratio of 0.31 measured by Ref. 19. Other works in indium-tin-oxide (ITO) have reported values of the Young's modulus of 103-190 GPa.[26,27]

Rods with hexagonal and rectangular cross section obtained by thermal decomposition of In_2S_3, as in this work, have been previously found to grow along the [111] and [100] directions, respectively.[28] This enables to compare the Young's modulus along both directions.[29] As can be seen, the Young's modulus in the [111] direction (rods A and B) is close to the value measured for the [100] direction, which is consistent with the high symmetric cubic system of indium oxide, in which no high anisotropies are expected. Besides, the similarity between Young's moduli values for both vibration directions in each rod is a good evidence for the lack of internal stress in the obtained structures.

The quality factor, hereinafter named as Q or Q-factor, of the microrods, calculated as $Q = \nu/2\gamma$, was estimated from the resonance curves by fitting the experimental data to Eq. (5). Q values in the range of 3780–1180 were obtained for different rods. Q-factors from few tens to 10^4 have been reported in the literature for simple resonant nano and micromechanical systems.[9,28,30–32] This makes In_2O_3 microrods a very promising material for the fabrication of resonant micromechanical devices such as sensors. Besides, the combination of high quality optical resonances, as reported recently for these In_2O_3 rods,[17] and the mechanical resonance properties reported here, could offer the possibility to increase their response through the optomechanical coupling, as reported for other systems by Vahala *et al.*[4,5] This recent application field will require for a more accurate measurements of In_2O_3 mechanical properties, as those reported here.

In order to compare the E values obtained by resonance frequency measurements and by force-displacement curves in AFM, the microrod A was also investigated by AFM. The microrod and its silicon substrate were transferred as a whole from the SEM to the AFM so that the rod was not subjected

to stresses or to any manipulation. The rod deflection induced by an applied force by the cantilever depends on the Young's modulus and the distance, x, from the tip of the cantilever to the fixed base of the rod. The linear relationship between force and displacement in a rod of constant section is given by[33]

$$\frac{dF}{dy} = \frac{3EI}{x^3} = k_r(x). \tag{6}$$

The fact that the slope of the elastic line is strongly dependent on x, can lead to errors in the estimation of E due to possible errors in the measurements of x. This effect is reduced by recording the elastic lines in different points along the microrod length and averaging the obtained E values. In particular, the measurements on microrod A were performed between 440 μm and 470 μm from the clamped end with 5 μm intervals. Figure 3 shows the force-displacement plot for $x = 450\ \mu$m. The straight line corresponding to elastic deformation is the result of bending of the system microrod–cantilever. The slope of this line, k, is related to the elastic constants of the cantilever, k_c (0.17 N/m) and the rod, k_r, by the following equation:[8]

$$k = \frac{k_r k_c}{k_r + k_c}. \tag{7}$$

The averaged E value for the microrod A obtained from the series of seven force-displacement curves along the rod is 158 GPa, which deviates about 8% from the Young's modulus determined by the resonance frequency method.

In summary, mechanical resonance induced by an alternating electric field in the chamber of a SEM has been used to measure the E modulus of In_2O_3 microrods with either hexagonal or rectangular cross sections. Also, moduli of microrods with constant cross section and with decreasing cross section from the base to the tip have been measured. The obtained E values were in the range of 131 GPa–152 GPa. This low dispersion of values indicates that the resonance method used is suitable to measure the elastic modulus of microrods with lateral dimensions of few microns and lengths up to the millimeter range.

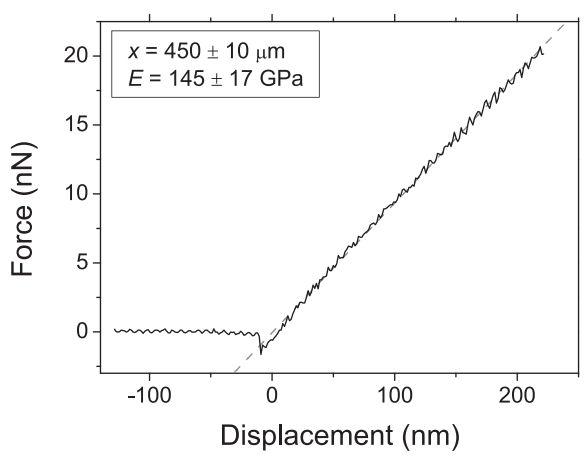

FIG. 3. Force–displacement curve recorded on the microrod A with an atomic force microscope. Linear fit to the force-displacement curve is shown by dashed line.

Measurements of E by force–displacement curves in AFM of the same microrod investigated by mechanical resonance, yielded 158 GPa which differs about 8% of the E value of 145 GPa measured by the resonance technique. These close E values show that the E values are representative of the structures investigated with no significant dependence of the technique used. A Q-factor range of 1180–3780 has been obtained for both rectangular and hexagonal cross-section rods during resonance measurements, showing that In_2O_3 microrods constitute a promising alternative material for fabrication of semiconductor micromechanical resonators.

This work has been supported by MINECO (Project Nos. MAT 2012-31959 and CSD 2009-00013). J.B. acknowledges the financial support from Universidad Complutense de Madrid.

[1]A. Boisen, S. Dohn, S. S. Keller, S. Schmid, and M. Tenje, Rep. Prog. Phys. **74**, 036101 (2011).
[2]J.-W. Han, J.-H. Ahn, M.-W. Kim, J. O. Lee, J.-B. Yoon, and Y.-K. Choi, Small **6**, 1197 (2010).
[3]E. Gil-Santos, D. Ramos, J. Martínez, M. Fernández-Regúlez, R. García, A. S. Paulo, M. Calleja, and J. Tamayo, Nat. Nanotechnol. **5**, 641 (2010).
[4]T. J. Kippenberg, H. Rokhsari, T. Carmon, A. Scherer, and K. J. Vahala, Phys. Rev. Lett. **95**, 033901 (2005).
[5]H. Rokhsari, T. J. Kippenberg, T. Carmon, and K. J. Vahala, IEEE J. Sel. Top. Quantum Electron. **12**, 96 (2006).
[6]G. Anetsberger, R. Rivière, A. Schliesser, O. Arcizet, and T. J. Kippenberg, Nat. Photonics **2**, 627 (2008).
[7]K.-K. Ni, R. Norte, D. J. Wilson, J. D. Hood, D. E. Chang, O. Painter, and H. J. Kimble, Phys. Rev. Lett. **108**, 214302 (2012).
[8]C. Röhling, M. Niebelschütz, K. Brueckner, K. Tonisch, O. Ambacher, and V. Cimalla, Phys. Status Solidi B **247**, 2557 (2010).
[9]X. D. Bai, P. X. Gao, Z. L. Wang, and E. G. Wang, Appl. Phys. Lett. **82**, 4806 (2003).
[10]C. Q. Chen, Y. Shi, Y. S. Zhang, J. Zhu, and Y. J. Yan, Phys. Rev. Lett. **96**, 075505 (2006).
[11]R. Agrawal, B. Peng, E. E. Gdoutos, and H. D. Espinosa, Nano Lett. **8**, 3668 (2008).
[12]M. Lucas, W. Mai, R. Yang, Z. L. Wang, and E. Riedo, Nano Lett. **7**, 1314 (2007).
[13]H. Ni and X. Li, Nanotechnology **17**, 3591 (2006).
[14]E. P. S. Tan, Y. Zhu, T. Yu, L. Dai, C. H. Sow, V. B. C. Tan, and C. T. Lim, Appl. Phys. Lett. **90**, 163112 (2007).
[15]Z. L. Wang, Z. R. Dai, R. Gao, and J. L. Gole, J. Electron Microsc. **51**(Suppl.), S79 (2002).
[16]H. Dong, Z. Chen, L. Sun, J. Lu, W. Xie, H. H. Tan, C. Jagadish, and X. Shen, Appl. Phys. Lett. **94**, 173115 (2009).
[17]J. Bartolomé, A. Cremades, and J. Piqueras, J. Mater. Chem. C **1**, 6790 (2013).
[18]J. J. Roa, G. Oncins, F. T. Dias, V. N. Vieira, J. Schaf, and M. Segarra, Physica C **471**, 544 (2011).
[19]K. H. L. Zhang, A. Regoutz, R. G. Palgrave, D. J. Payne, R. G. Egdell, A. Walsh, S. P. Collins, D. Wermeille, and R. A. Cowley, Phys. Rev. B. **84**, 233301 (2011).
[20]See supplementary material at http://dx.doi.org/10.1063/1.4872461 for videos and a more detailed description of the deflection of the rods with the electric field.
[21]S. Timoshenko, *Vibration Problems in Engineering* (D. Van Nostrand Company Inc., New York, 1937).
[22]H. E. Schoeller, M.S. dissertation, Binghamton University, 2007.
[23]A. Walsh, C. Richard, A. Catlow, A. A. Alexey, A. Sokol, and S. M. Woodley, Chem. Mater. **21**, 4962 (2009).
[24]D. Liu, W. W. Lei, B. Zou, S. D. Yu, J. Hao, K. Wang, B. B. Liu, Q. L. Cui, and G. T. Zou, J. Appl. Phys. **104**, 083506 (2008).
[25]F. Fuchs and F. Bechstedt, Phys. Rev. B. **77**, 155107 (2008).
[26]T. Wittkowski, J. Jorzick, H. Seitz, B. Schröder, K. Jung, and B. Hillebrands, Thin Solid Films **398–399**, 465 (2001).

[27]B.-K. Lee, Y.-H. Song, and J.-B. Yoon, in *IEEE 22nd International Conference on Micro Electro Mechanical Systems, 2009* (IEEE, 2009), p. 148.
[28]W. Ding, L. Calabri, X. Chen, K. M. Kohlhaas, and R. S. Ruoff, Compos. Sci. Technol. **66**, 1112 (2006).
[29]C.-H. Lin, H. Ni, X. Wang, M. Chang, Y. J. Chao, J. R. Deka, and X. Li, Small **6**, 927 (2010).
[30]K. Brueckner, F. Niebelschuetz, K. Tonisch, C. Foerster, V. Cimalla, R. Stephan, J. Pezoldt, T. Staunden, O. Ambacher, and M. A. Hein, Phys. Status Solidi A **208**, 357 (2011).
[31]J. Lee, Z. Wang, K. He, J. Shan, and P. X.-L. Feng, ACS Nano **7**, 6086 (2013).
[32]M. J. Burek, D. Ramos, P. Patel, I. W. Frank, and M. Lončar, Appl. Phys. Lett. **103**, 131904 (2013).
[33]E. W. Wong, P. E. Sheehan, and C. M. Lieber, Science **277**, 1971 (1997).